Examining Open-Top Culverts Impact on Forest Road Surface Deteriorations via UAVs

Yılmaz Türk, Abdurrahim Aydın, Remzi Eker

Abstract

The life and robustness of forest roads depend on their protection from the harmful effects of water coming into the road surface. In particular, the deterioration of the road surface affects the safe navigation of vehicles and traffic safety. This situation requires that the surface be stable on forest roads. The aim of the study is to examine whether surface deterioration (erosion and accumulation) on forest roads due to the drainage problem of water falling on the road surface can be minimized by open-top culverts and to determine their effectiveness. These are used in three separate trial blocks every 25 m (A parcels; total of 3 parcels), every 50 m (B parcels; total of 3 parcels) and control block (C). Volumetric erosion and accumulation in these blocks was compared by UAV for about 3 years and the effectiveness of the open-top culverts was examined by this method. A 500 m section of the forest road coded 001 of the Kardüz Forest Operations Directorate (Düzce/Türkiye) was examined in the study. As a result, erosion and accumulation in all blocks have been found to have a dynamic course. It was determined that this mobility was greater in the control block than in the blocks with open-top culverts installed at intervals of 25 m and 50 m. The mean Z values for the blocks showed that the deterioration in the control block (C) was higher than in the blocks with 25 m and 50 m open culverts. The volumetric deterioration rate was 5 times higher in the control block than in the block installed at 25 m interval (A plots) and 2 times higher than in the block installed at 50 m interval (B plots). Similarly, the areal deterioration rate was 3.3 times higher in the control block than in the block installed at 25 m interval (A plots) and 1.4 times higher than in the block installed at 50 m interval (B plots). These results showed the effectiveness of open-top culverts and it was also determined that the open-top culverts installed at 25 m intervals were more effective than the open-top culverts established at 50 m intervals. In addition, according to the statistical analysis, a statistically significant difference was found between the erosion volume in the blocks. Open-top culverts should be used against forest road surface deterioration and UAV technology should be used for deterioration detection.

Keywords: forest road, open-top culverts, drainage, erosion, accumulation, UAV

1. Introduction

Ensuring the continuity of the road surface (pavement), especially on forest roads, by keeping the deterioration to a minimum, ensures that the road is open to access for many years and reduces maintenance and repair costs (Bayoğlu 1997, Kramer 2001). In addition, the cost of building forest roads is considerable, even when relatively cheap materials such as aggregates of natural or anthropogenic origin are used (Grajewski 2023). Road surface is one of the most important elements to ensure the continuity of the functions that forest roads will perform during the service period

and to maintain safe vehicle traffic and driving dynamics (Haas 2001, Morgado and Neves 2014, Lee et al. 2015, Akay 2018). The forest road consists of two main sections: infrastructure and road surface. The infrastructure consists of excavation and filling and architectural structures (bridge, retaining wall, culvert), while the road surface consists of the lower base and the basic layers exposed to traffic load (Bayoğlu 1997, Erdaş 1997, AASHTO 2001, GDF 2008, Adlinge and Gupta 2013, BCMF 2018).

Road surface deterioration is the process by which distress (defects) develop in the surface under the combined effects of traffic loading and environmental

conditions (Adlinge and Gupta 2013). The road surface built on the infrastructure deteriorates over time due to climate effects (Fwa 2005, Wee and Teo 2009, Akgul et al. 2017, Akgul et al. 2019), traffic load (Tighe et al. 2003, Zhang 2008, Kaare et al. 2012, Boghian et al. 2015, Akgul et al. 2019, Yurtseven et al. 2019), maintenance done (Haas 2001, Tighe et al. 2003), materials used (Adlinge and Gupta 2013), poor drainage (Abhijit and Jalindar 2011) and other environmental factors (George et al. 1989). There are three fundamental mechanisms of deterioration: wear and abrasion of the road surface material under traffic, deformation of the surface and roadbed material under the stresses induced by traffic loading and moisture conditions, and, finally, erosion of the surface by traffic, water and wind (Paterson 1987). Deterioration types are generally determined according to road surface defects; these are divided into three main sections: cracks, separations and permanent deformation (Paterson 1987, Kramer 2001, Haas 2001). Although these three main sections are reserved for highways, there is also general decomposition and deformation on forest roads (Paterson 1987).

The methods used to detect and measure the deterioration in the road surface are divided into two categories: traditional (manual) and automatic methods. Both methods differ in time, security, objectivity, cost, data size, data management, and scope (Attoh-Okine and Offei 2013). Automated methods have entered the highway literature because they measure deteriorations more precisely and limit the disadvantages of the traditional method (Herr 2001, Wang 2005, Chang et al. 2005, Herr 2009, Li et al. 2009, Wang et al. 2011, Huang et al. 2011, Tsai et al. 2013). UAV systems, which are one of the remote sensing techniques, are automatic methods and are frequently used today.

Nowadays, UAV technology is frequently used except for roads and close results are obtained with field measurement results. UAVs are used in studies such as volume calculation related to land surface change (Ulvi 2018, Gülci and Kılınç 2018), monitoring of rockfall area (Yakar et al. 2023), landslide areas and production of a landslide inventory map (Kusak et al. 2021), monitoring and volume calculation of soil erosion on fairy chimneys (Yilmaz et al. 2012), estimating the size of soil deterioration after wood harvesting (Talbot et al. 2018).

Photogrammetry methods are also used to determine deteriorations, such as erosion occurring on roads. In a study on the determination of road surface deteriorations, photogrammetric methods were applied to store, record, process, and reduce surface data in order to minimize errors and standardize the surface survey process (Attoh-Okine and Adarkwa 2013). The

first study on roads using photogrammetric methods was carried out by Zhang (2008) to assess the condition of soil roads. In this study, data acquisition was performed with a UAV at a height of 50 m above the ground. Díaz-Vilariño et al. (2016), on the other hand, compared the photogrammetric data quality obtained using UAVs with the data obtained using a mobile LIDAR system on an asphalt road in a mountainous area and evaluated their effects on the detection of runoff on the road surface. Hrůza et al. (2016) demonstrated the possibility of detecting and monitoring the wearing course of forest roads with UAVs. Dobson et al. (2013) also recognized the need for effective periodic monitoring of a soil (unpaved) road and conducted a study on monitoring road deteriorations (such as washboarding, cracking, potholes and cross-sectional deformations of the road platform) using a UAV-based approach.

Furthermore, Hasegawa et al. (2023) used UAVs to calculate the earthwork volume of a road repair work and stated that UAVs can be used to accurately calculate the earthwork volume. Apart from these studies, UAV systems have also been used in road classification (Biçici and Zeybek 2021). In the literature, there are studies (Hrůza et al. 2016, Gülci and Şireli 2019, Cheng et al. 2023, Eker 2023, Türk et al. 2024) in which close-range photogrammetry is also used for the determination of forest road surface deterioration.

In studies on forest roads in Turkey, Akgül et al. (2017) evaluated meteorological conditions, which have an effective role in deteriorations occurring in the forest road surface, using a local laser scanner. Türk et al. (2018) evaluated the possibilities of using UAVs to determine the environmental impacts of forest road construction activities. In the study, it was stated that optical sensors have limited capabilities in areas with high stand density for mapping the fill area and construction impact area due to road construction. Furthermore, in their study, Buğday (2018), Ciritcioğlu and Buğday (2022), Kınalı and Çalışkan (2022) and Türk et al. (2022a) examined the ability to use UAV in determining the cut and fill volumes in the construction of forest roads. In these studies, it was emphasized that UAV technology is effective in forest road volume calculations.

Hrůza et al. (2016) presented in their study that it is possible to detect deterioration with a 2 cm RMSE (root mean square error) using UAV data. Yurtseven et al. (2019) emphasized that in a point cloud-based study on forest road surface modeling, the road surface models obtained with a terrestrial laser scanner and UAV were close to each other in terms of precision and that UAV systems can be used on forest roads. Recent studies on UAV-based monitoring of road

surface deteriorations were carried out by Türk et al. (2019a, 2019b) and Türk et al. (2022b). In addition, Türk et al. (2024) used UAVs to detect surface erosion on the excavation slope. In these studies, deteriorations on the forest road were detected by the UAV and its usability was stated. In our study, UAV technology was used as in other studies. However, in our study, the effectiveness of open-top culverts was investigated with a UAV for the first time. In addition, unlike other studies, an algorithm was used in the volume calculation of forest road surface deterioration.

Raindrops falling on the road surface, where the longitudinal slopes of forest roads, which are usually located in mountainous terrain, are high, constantly flow along the road axis and do not immediately leave the road surface. This water, whose flow rate increases with the effect of the slope, plays on the road surface over time and then causes the formation of fissures. This formation gains even greater speed as the road slope increases. For this reason, the waters that cause damage by flowing along the road axis on forest roads are removed from the road surface with open-top culverts of various shapes (Bayoğlu 1997, Erdaş 1997).

Open-top culverts are only used for forest roads. Open-top culverts are manufactured in different sections with steel and concrete materials other than wood (Fig. 1). Wooden open-top culverts can also be made of round trees and uniformly cut planks.

This study assesses the impact of open-top culverts on forest road surface deterioration using UAV technology. In determining the effectiveness of open top culverts, erosion and accumulation volumes on the road surface were analyzed as deterioration. In this context, in order to determine the deterioration caused by rainwater on the surface of sloping (9%) forest roads, wooden open-top culverts were placed at different intervals on the road surface. In addition, the deterioration rate was determined in 25 m (A parcels), 50 m (B parcels) and control (C) blocks where open-top culverts were installed with high precision with the UAV. In the study, the relationship between the deterioration in the blocks with open-top culverts installed at 25 m and 50 m intervals and the deterioration rates in the control block was subjected to statistical analysis. Apart from the open-top culverts in the study, the UAV (Drone), which has been used and accepted in international literature in recent years, has been used to analyze deterioration on forest road surfaces and produce a high-resolution orthophoto map. Thus, road surface maintenance works, which is a costly process, were carried out where necessary (on the local forest road surface instead of the complete road surface) to reduce road repair and maintenance costs and to determine the road surface material required for road repairs with high precision.
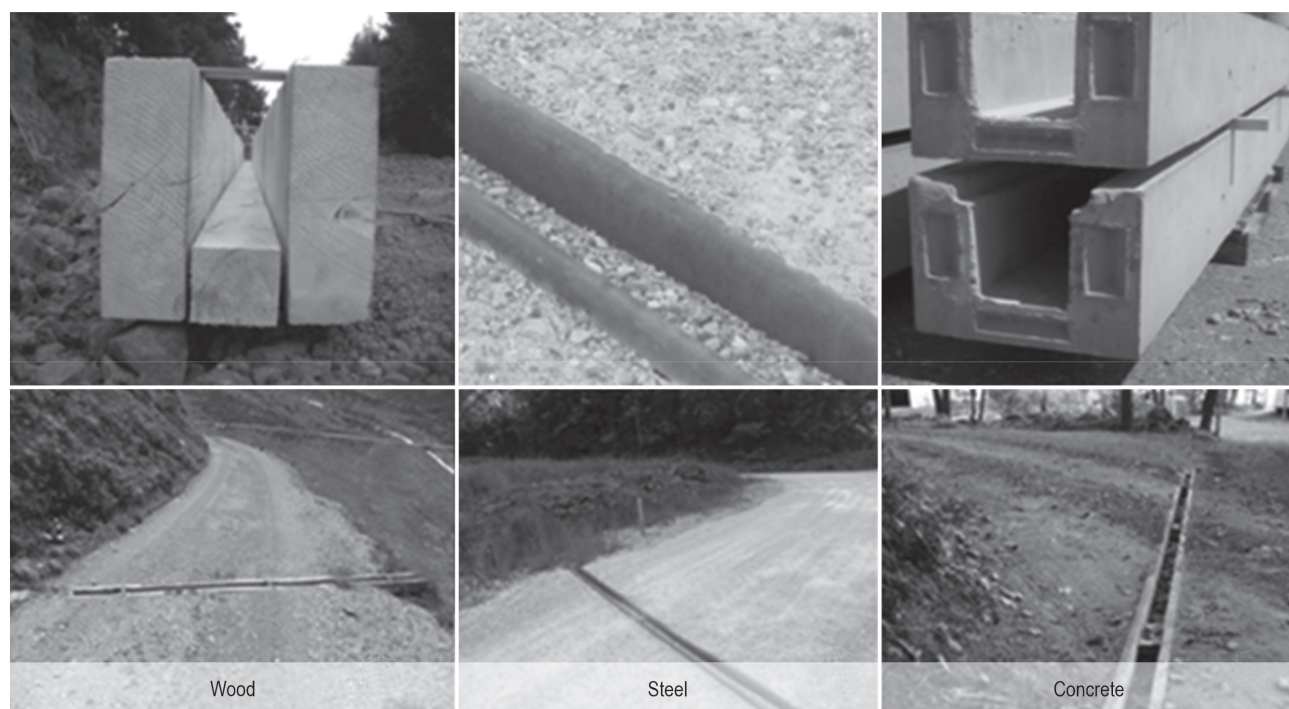

Fig. 1 Open-top culverts and their deployment

2. Materials and Methods

2.1 Study Area

As a field of study, the first 500 meters of the forest road with the code 318 in Kardüz Forest Operations Directorate (FOD) (Düzce/Turkey), which is open to wood transport and recreational vehicle use and of which 2 km of surface was renewed in August 2017, was selected. The Kardüz Region is located in the Western Black Sea Region between 40° 39' and 40° 45' north latitudes and 30° 53' and 31° 01' east longitudes (Fig. 2). Kardüz FOD has a total area of 5045 ha, of which 3745 ha are forested and 1300 hectares are unforested. Approximately 87 km of forest roads are found in Kardüz FOD. According to the Kardüz Plateau Meteorological Station, the average annual rainfall is 840 mm, and the average annual temperature is 13 ⁰C. The main tree species of the region are Eastern Beech (Fagus *orientalis* Lipsky.), Uludağ Fir (Abies *nordmanniana* subsp. *bornmülleriana* Mattf) and Yellow Pine (Pinus *sylvestris* L.) (GDF 2011).

2.2 Applications of Wooden Open-Top Culverts

Following the renewal of the surface in August 2017 on 2 km of the forest road coded 318, which is the subject of the study, wooden open-top culverts were placed in the area. All of the open-top culverts used in this study were formed from uniformly cut planks. Two side planks, 10 cm thick and 25 cm wide, form the culvert sides, and an 8 cm thick, 10 cm wide (= free opening) base plank forms the bottom of the culvert. The section of the culvert is fixed on the lower side and upper side with clamping bands made of ferrous iron on the lower side to form a rectangle. The wooden open-top culvert prepared in this way was placed in a trench 30–40 cm wide and 4–5% inclined at a 30-degree angle to the road axis at the place where the culvert would be fixed, and the sides were compressed with crushed stone and gravel (Fig. 3).

A total of 3 blocks were formed on the 500 m section of the road subject to the study, and a total of 7 wooden open-top culverts were used. The deterioration of the selected blocks as one in 25 m (3 parcels: A1,
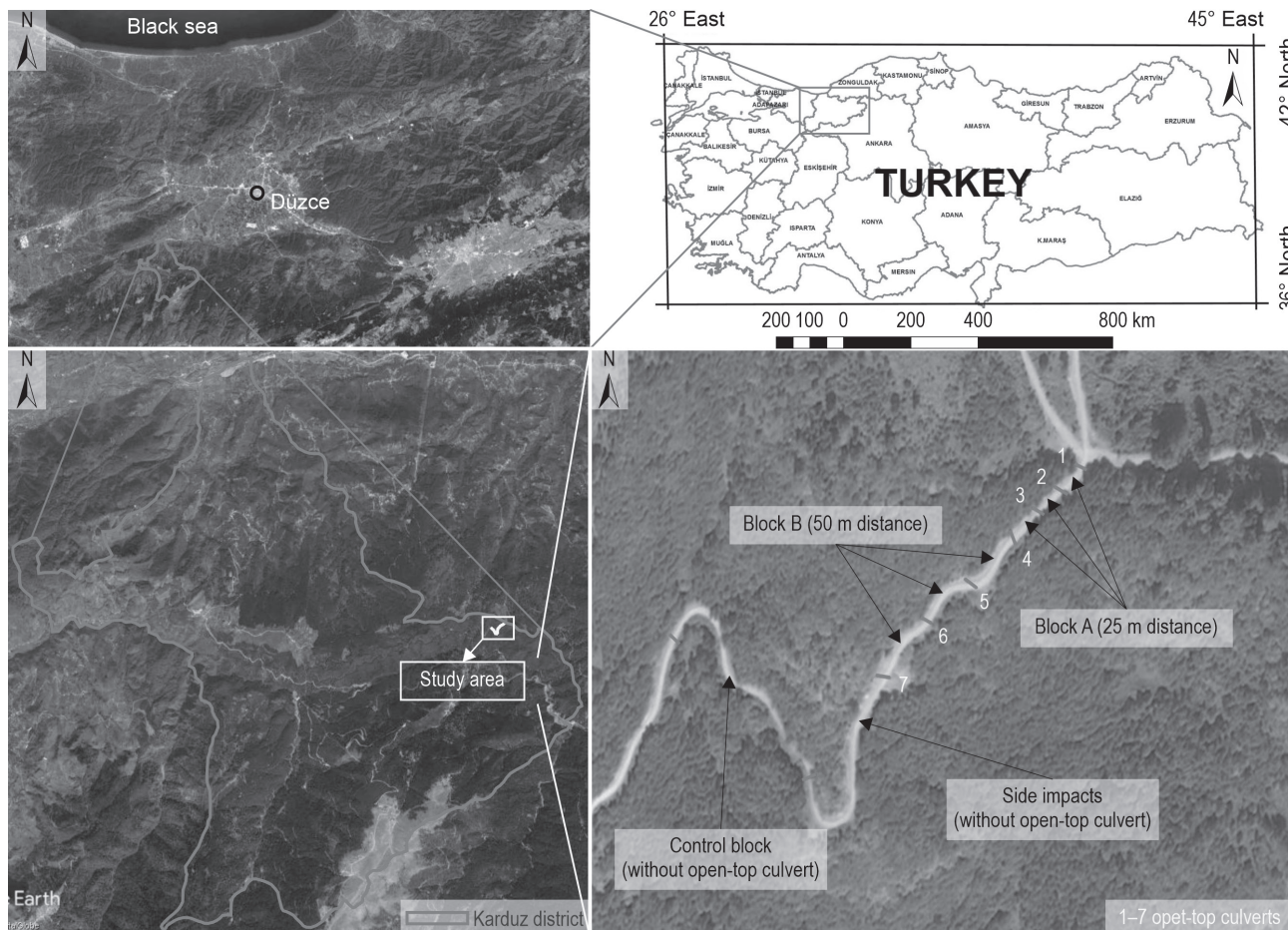

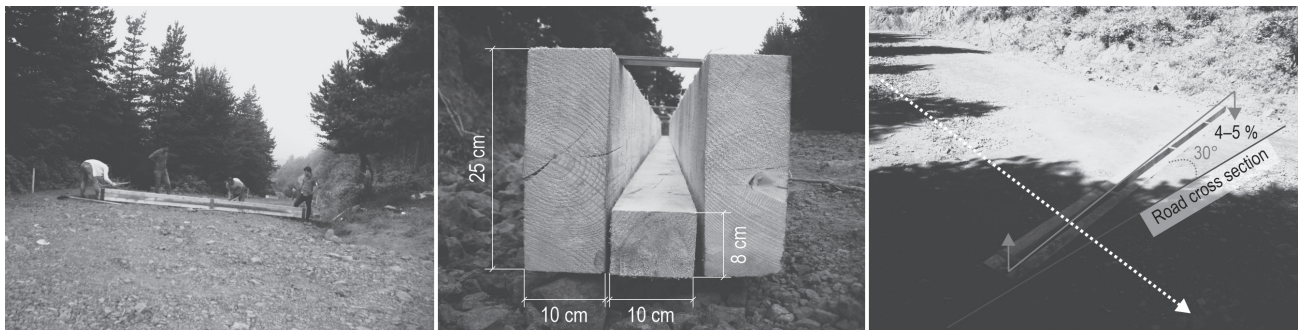**Fig. 2** Study area and surroundings

Fig. 3 Design of open-top culverts used in this study

A2, A3) on the first block (A), one in 50 m on the second block (B) (3 parcels: B1, B2, B3), and a third control block (C) (125 m) were examined. In addition, the part between B3 and C was left empty due to side impacts (SI) (150 m). Attention was paid to the fact that the geometric features of the road in the selected blocks (approximate road longitudinal gradient: 9%, average width of the road: 4 m), were the same.

2.3 Acquisition of UAV Digital Images

In order to monitor the deterioration in the road surface and to evaluate the effectiveness of the deployed open-top culverts, it was aimed to create high-accuracy and high-resolution orthophoto mosaics using the UAV and the Digital Elevation Models (DEM). As a UAV platform, two platforms were used in the study: the DJI Mavic Pro model until April 17, 2020, and the DJI Phantom 4 RTK system after that date. The DJI Mavic Pro model has an integrated 12-megapixel resolution camera. The flights on the road surface were planned using UgCS flight planning software as an adaptive topography that allows images to be taken with a fixed 1.5 cm terrestrial resolution. In this context, a flight plan was created with 70% front and side overlap, 48 m AGL (above ground level) altitude above ground level, and lasting an average of 15 minutes.

The other UAV platform, the DJI Phantom 4 RTK system, was used on April 17, 2020. This model is more advantageous than the other in terms of workload (decrease in the number of ground control points) and image resolution. The DJI Phantom 4 RTK system features a 1-inch, 20-megapixel CMOS sensor. It has a global navigation satellite system (GNSS) receiver that allows for multi-frequency RTK data reception and provides high position accuracy on the UAV system.

The flight planning process was created under the control of the DJI Phantom 4 RTK system with the DJI GS RTK application. In this context, firstly, the DEM data of the field (SRTM DEM 30 m resolution) and a vector of data covering the boundaries of the flight area (in KML format) were transferred to the control with an SD card. Then, using this data, taking into account the size of the area and the duration depending on the battery capacity of the UAV, the topography with 75% front and side overlay rates was done in a way to make an adaptive flight. The topography of the road platform was planned using UgCS flight planning software as an adaptive topography that allows images to be taken with a fixed 1–1.3 cm terrestrial resolution. In this context, an average flight plan of 15 minutes was created at 60 m AGL (above ground level) with a 70% front and side overlay.

Before the realization of DJI Mavic Pro platform flights in the field, 42 ground control points (GCPs) were applied onto the road platform, which can be clearly seen in the images to be taken with the UAV. In the flights on the DJI Phantom 4 RTK platform, 12 GCPs were applied to the broken points of the road. The X, Y, and Z coordinates of each GCP in the TUREF TM30 coordinate system, which were applied with red spray paint on the road surface, were measured with a SATLAB SL600 6G RTK GNSS receiver with 1–2 cm error horizontally and vertically. Following the completion of the application of GCPs to the area, flights were carried out. In addition, in order to find the obtained pixel values, buckets of a certain height were placed on the road surface and the flights were carried out in this way. Thus, it was determined which threshold value would be filtered to determine the volume of erosion or accumulation.

In the study, the first UAV flight was carried out on September 9, 2017 after the completion of the deployment of the open-top culverts on the road (August 30, 2017). The study data covered more than 3 years of results (September 2017 – November 2020), and a total of 20 flights were made within the scope of the working period. Flights were not made when the road was covered with snow. Within the scope of post-flight

office work, the images taken by the UAV were processed and the cloud point of high resolution and accuracy found. Agisoft Metashape Professional Version 1.5.2 software was used to produce DEM and orthophoto images. The software was run on the Windows 10 64-bit operating system. While the accuracy level of the image routing process was set to medium, the quality settings were high in other depth map production, dense cloud generation stages; the quality settings were also selected as high. The output produced as a result of photogrammetric analysis of the images is dense point cloud data in ».las« format, DEM and orthomosaics in ».tiff« format. Then, in order to ensure areal consistency in the analyses, all DEM and orthomosaics were reduced to the same size by using vector data representing the working area in ».shp« format.

2.4 Determination of Road Surface Deterioration

In the study, deteriorations on the road surface were evaluated using the change in Z values for each block. Here, all pixels within the polygon of each block digitalized in the GIS software were not used because of the presence of vegetation in the area close to the edge ditches, wood raw material left on the roadside after harvesting operations carried out in the field, and the presence of rock fragments aside from the usual deterioration processes of the road. The aim of this was to use the Z values of the pixels that are within these selected zones and whose usual deterioration was not affected by external factors. Each flight data was checked before the volume calculation, and before any of these factors were taken into account. In this way, measurement errors were prevented, and accuracy was obtained in calculations between periods. In this context, the importance of Z-value differences has increased.

In order to correctly analyze the ordinary deteriorations, points were placed in the areas close to the middle line of the road surface at certain intervals depending on the length within each block, and then circle-shaped zones (buffers) with a radius of 50 cm were defined at these points. The aim of this was to use the Z values of the pixels that are within these selected zones and whose usual deterioration was not
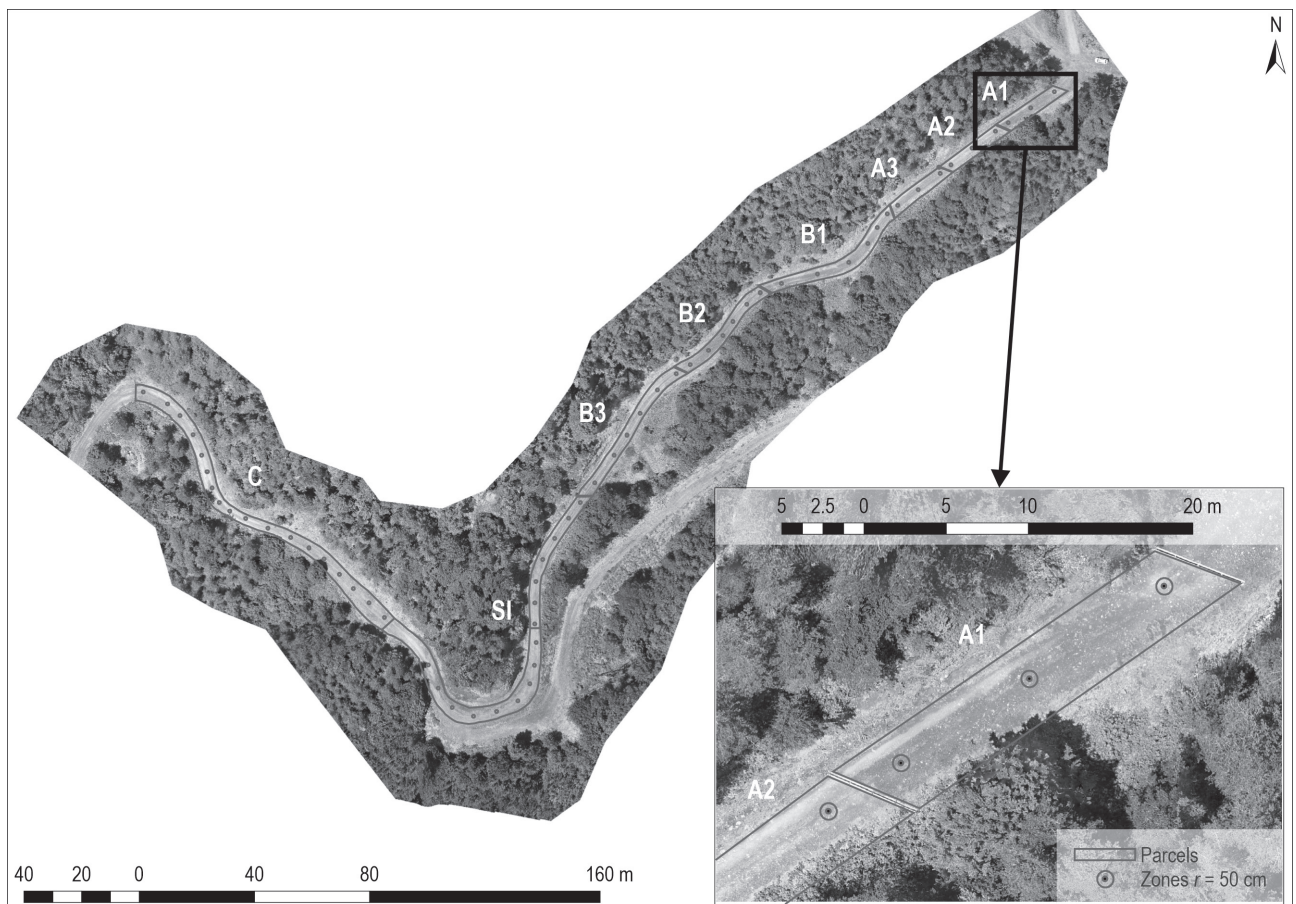

Fig. 4 Circular zones with a 50 cm radius defined in each block on the road surface

affected by external factors. These points defined on the road surface in the study are shown in Fig. 4.

Deteriorations within the determined zones were determined by using the average Z value of all pixels in the zone. The average Z values of the pixels were determined for all flights using the zonal statistics tool (ArcMAP-Sapatial Analyst-Zonal Statistics Tool). Then, based on the first flight data dated September 9, 2017, the differences in the average Z value obtained from other flights (19 PCs) were determined. In the study, it was important to define the zones and determine the average Z value of the pixels in them because, if the Z value of only a single pixel were taken into account, errors could occur in the modeling process due to reasons such as flight height, image quality, or shadow effect, and therefore cause misleading results. For each block, scatter blocks were produced by using the differences in the mean Z values of the zones in it, and the deteriorations were compared. Thus, the effectiveness of open-top culverts on the deteriorations in the relevant blocks could be evaluated more accurately.

During the study, 2D analysis was also carried out to determine the volume and areal of the material that was deformed and accumulated in the blocks. In this context, DEM differences were taken first (Fig. 5a). In this process, DEM is applied by subtracting the value of each pixel forming the DEM data produced in raster format (in DEM, this value is the height above sea level) from the value of the overlapping pixels of the other DEMs in the time series. DEM differences were subtracted from other flights based on the first flight data dated September 9, 2017. The block boundaries were cut out from the different DEM data (Fig. 5b) produced as a result of this process. Then, the volumetric and areal determination of the deterioration was carried out separately for each block, free from external factors. In order to determine the volume and areal an add-on in the form of a toolbox was designed into the ArcMAP module of the ArcGIS software with the Python programming language (Fig. 5c). From the DEM difference data, the algorithm calculates the volume and areal accumulated over all pixels with positive difference values and the volume and areal eroded over all pixels with negative values, as shown in Fig. 5d. The algorithm records the volume and areal information as a text file (.txt extension) in the location defined as the workspace (Fig. 5e) (Türk et al. 2022a). The algorithm uses the DEM of difference data. In this data, the operation is performed on the value of the pixels. If the pixel value is less than 0, it is considered erosion; if it is larger, it is considered accumulation.
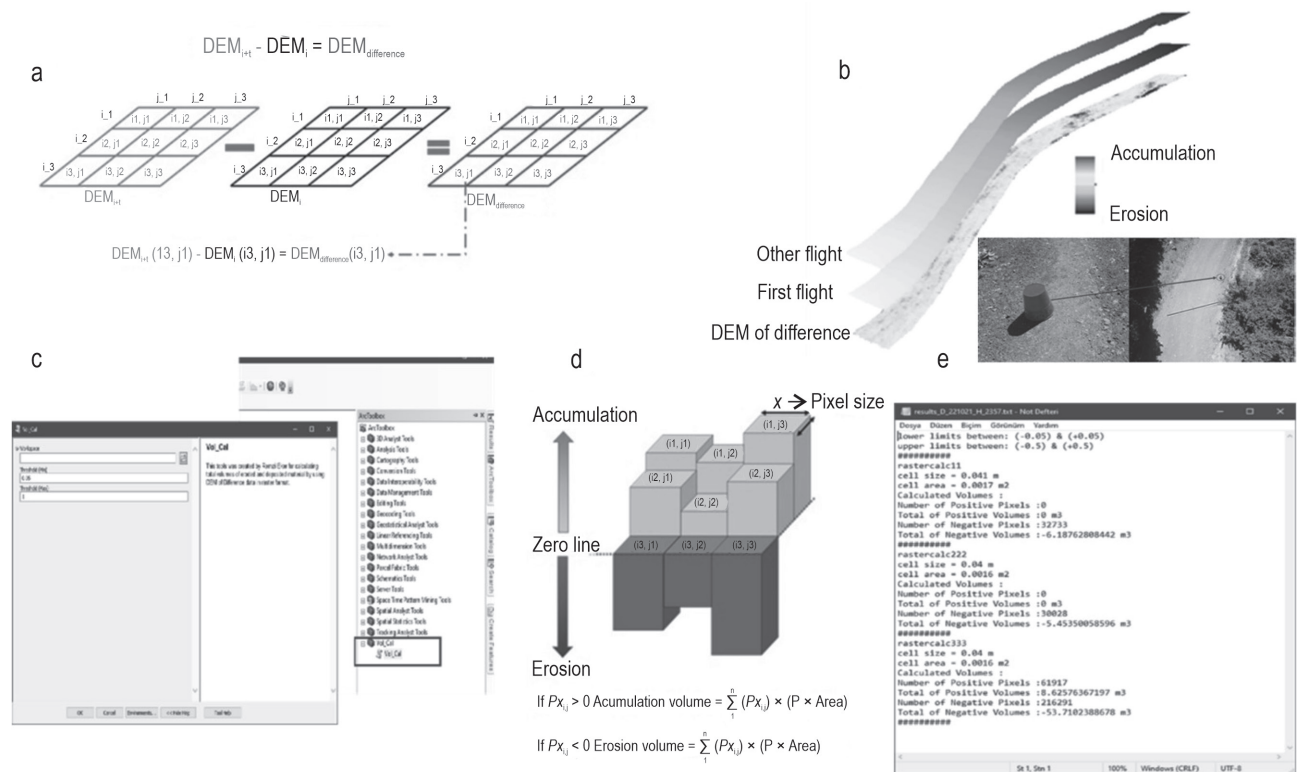

Fig. 5 Analyses for the determination of volumetric and areal deterioration

The volume in each pixel is calculated by multiplying the pixel area depending on the resolution by the value of the pixels with erosion or accumulation, and the total volume is obtained. The total size of the pixels with erosion or accumulation gives the overall results.

The accuracy of the algorithm is also related to the accuracy of the UAV models. When calculating erosion and accumulation, the algorithm applies the threshold value using model errors. For example, if the model errors are X cm, pixels in the range ±X cm are not included in the volume calculation. This difference is seen as a modeling error. If the pixel value in the difference data is outside this range, it is considered deterioration. For this reason, buckets of certain height and volume were placed on the road platform to find the pixel values obtained in the study, and the flights were carried out in this way. Thus, it was determined between which values the surface deterioration should be filtered (Fig. 5b). In addition, deterioration, volumetric, and areal maps were created by classifying the deteriorations in separate tabs with ArcGIS software. Similarly, each flight data was checked before the volume calculation, and the unusual factors were digitized in GIS software and removed from the study area. In such cases, random forest, support vector machine , etc. algorithms can be used for path extraction and external factor filtering.

2.5 Statistical Methods Used

The Kolmogorov-Smirnov normal distribution test was used to investigate whether the data was normally distributed or not. When the data did not show a normal distribution, necessary changes were made to ensure a normal distribution. Analysis of variance was applied to find out whether there was a difference in the volumetric deterioration per square meter and Z differences between the blocks. The Z differences in the blocks were normalized for statistical analysis due to the presence of negative values. The normalization formula is given below. Here, it is used to calculate the position of each value relative to the highest and lowest values in a population. All statistical analyses were carried out with the SPSS 22 package program.

Normalization formula:

$$X' = \frac{X - X_{min}}{X_{max} - X_{min}} \tag{1}$$

3. Results

3.1 Findings about Road Surface Deteriorations

The average width of the road subject to the study was 4 m and the approximate longitudinal gradient was 9%. Within the scope of the study, the deterioration of the road surface in the blocks was monitored with UAV flights for a period of about 3 years. The images obtained were georeferenced, a point cloud was created with the SfM algorithm, and then the DEM and orthophoto production of the road were carried out. In the DEMs of the road, the lowest land elevation was calculated as 1146 m and the highest land elevation as 1198 m.

Within the scope of the study, two methods were applied to evaluate the effectiveness of open-top culverts on road surface deterioration. The first of these was to compare the differences in the mean Z values of the pixels within the defined zones at certain intervals in the regions close to the road surface centerline in each block on the road. Within the scope of the study, the second method of evaluating the effectiveness of open-top culverts on road surface deterioration was to evaluate the volume and areal of the material erosion and accumulation within the determined blocks.

3.1.1 Findings on Z Value Differences in the Blocks

Within the scope of the study, the first of the methods applied to evaluate the effectiveness of open-top culverts on road surface deterioration was to compare the differences in the mean Z values of the pixels within the defined zones at certain intervals in the areas close to the road surface center line within each block on the road. The purpose here was to prevent misleading effects, especially the presence of vegetation in the areas close to the side ditches of the road (branch-leaf and living cover), the products left on the road as a result of the road works in the area and the presence of rocks or stones other than those from the usual deterioration process. In this method, the average Z values in the zones were compared by producing distribution charts for each block. Table 1 presents the average Z values for the blocks, and the graphs obtained from these operations are given in Fig. 6.

When Table 1 and Fig. 6 are examined, as expected, the deterioration obtained from the flight data in the control block (C) is higher than that in the blocks with 25 m (A1, A2, and A3) and 50 m (B1, B2, and B3) open-top culverts. In the study, in order to eliminate the unusual effects that influence road surface deterioration, it was ensured that the results were obtained in a more trustworthy way by using the method mentioned here. The change indicated here as distortion is the difference in the average Z values of the pixels. The size of the areas exposed to erosion or accumulation and the volumetric status of the eroded or accumulated material are not taken into account.

Table 1 Average *Z* differences on each block from DEM differences

DEM difference between flights	*Z* differences on blocks, m						
	A1	A2	A3	B1	B2	B3	C
Sep. 2017 – Nov. 2017	–0.08	0.01	0.03	–0.03	–0.06	–0.05	–0.10
Sep. 2017 – Apr. 2018	–0.08	–0.01	0.06	0.03	–0.06	–0.11	–0.03
Sep. 2017 – Nov. 2018	0.03	0.09	0.04	–0.02	–0.07	–0.01	–0.12
Sep. 2017 – Mar. 2019	–0.05	0.01	0.05	0.05	–0.01	–0.06	–0.07
Sep. 2017 – Apr. 2019	–0.03	0.03	0.06	0.02	–0.03	–0.10	–0.09
Sep. 2017 – May 2019	–0.04	0.03	0.05	0.03	–0.04	–0.12	–0.10
Sep. 2017 – June 2019	–0.04	–0.01	0.01	0.05	–0.06	–0.11	–0.14
Sep. 2017 – July 2019	–0.06	–0.03	0.01	0.03	–0.08	–0.09	–0.06
Sep. 2017 – Aug. 2019	–0.07	–0.03	–0.01	0.02	–0.03	–0.11	–0.07
Sep. 2017 – Sep. 2019	–0.02	–0.01	0.01	0.00	–0.03	–0.09	–0.09
Sep. 2017 – Nov. 2019	0.00	0.03	001	0.01	–0.01	–0.07	–0.08
Sep. 2017 – Apr. 2020	–0.04	–0.02	0.00	0,01	–0.02	–0.08	–0.10
Sep. 2017 – May 2020	–0.06	–0.03	0.01	–0.02	–0.06	–0.10	–0.08
Sep. 2017 – June 2020	–0.08	–0.01	0.02	0,00	–0.03	–0.14	–0.02
Sep. 2017 – July 2020	–0.14	0.02	0.01	–0.03	–0.06	–0.07	–0.14
Sep. 2017 – Aug 2020	–0.09	–0.04	–0.01	–0.05	–0.17	–0.23	–0.21
Sep. 2017 – Sep. 2020	–0.11	–0.04	0.01	–0.01	–0.05	–0.11	–0.12
Sep. 2017 – Oct. 2020	–0.06	0.02	0.06	0.01	–0.05	–0.10	–0.11
Sep. 2017 – Nov. 2020	–0.06	–0.01	0.01	0.00	–0.05	–0.08	–0.14

3.1.2 Volumetric and Areal Findings of Erosion and Accumulation on Blocks

In the study, the second method of evaluating the effectiveness of open-top culverts on road surface deterioration was to evaluate the erosion in the blocks determined by vector data. In the same way, as with the *Z* differences, the presence of vegetation in the blocks, post-roadworks waste and the rock or stone fragments coming into the road, aside from the usual deterioration processes of the road, were removed and cleared of external factors. The erosion and accumulation volumes of each block by years are given in Table 2

Table 2 Volumetric erosion and accumulation from DEM differences on blocks

| DEM difference between flights by year	Volumetric erosion (–) and accumulation (+) on blocks, m³													
	A1		A2		A3		B1		B2		B3		C	
	(–)	(+)	(–)	(+)	(–)	(+)	(–)	(+)	(–)	(+)	(–)	(+)	(–)	(+)
First Year Sep. 2017 – Nov. 2018	0.843	4.819	0.001	6.643	0.125	1.743	3.007	1.452	7.634	0.094	2.511	1.748	62.804	10.698
Second Year Sep. 2017 – Nov. 2019	1.979	2.934	0.635	2.406	0.124	2.145	1.123	1.953	2.330	1.093	10.141	0.047	43.032	12.114
Third Year Sep. 2017 – Nov. 2020	3.296	0.047	0.720	0.276	0.126	0.727	1.165	0.472	5.680	0.128	12.292	0.049	60.963	2.430
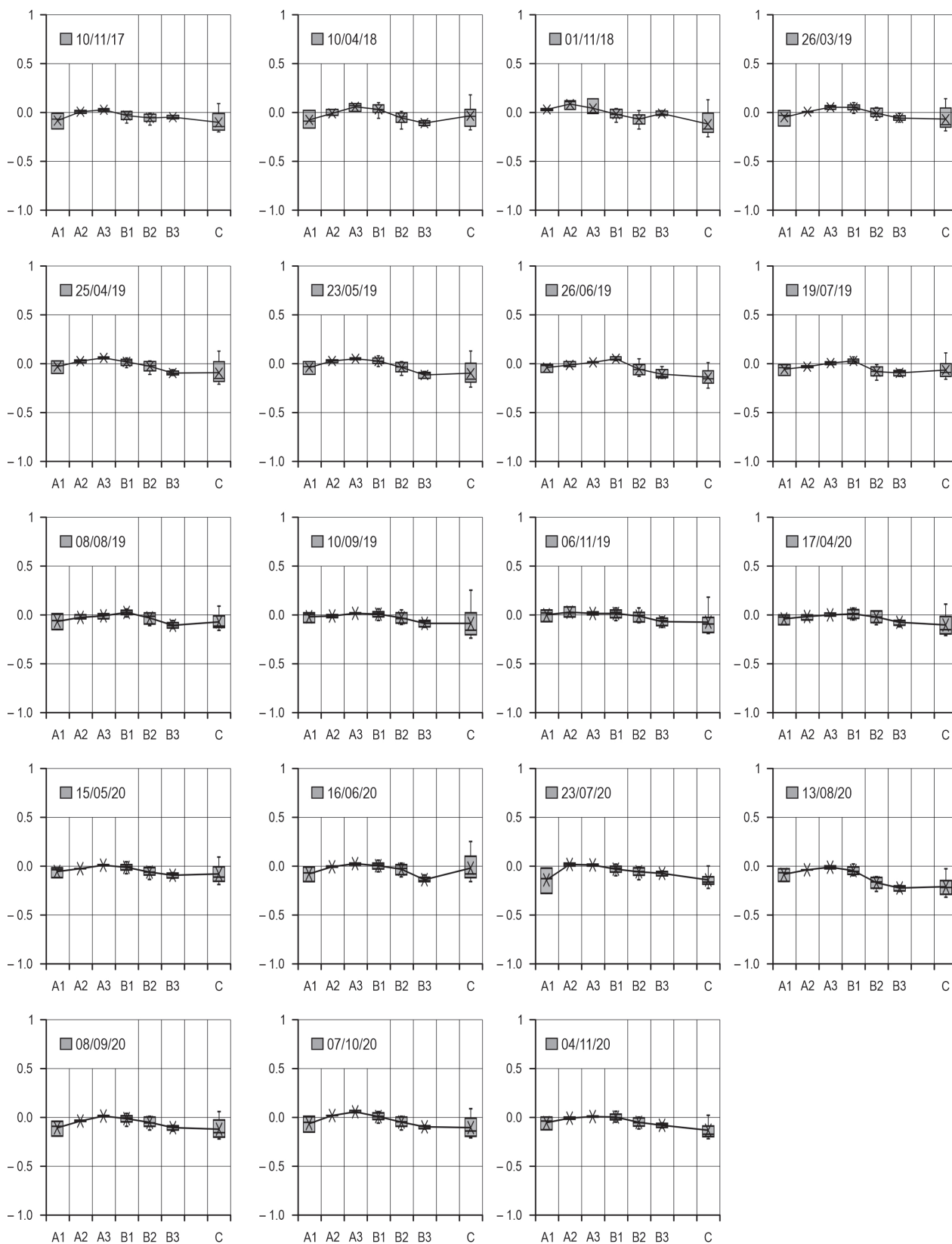
Fig. 6 Deteriorations derived from differences in average *Z* values in each block using flight data (vertical axis are *Z* difference values in the graph, m)
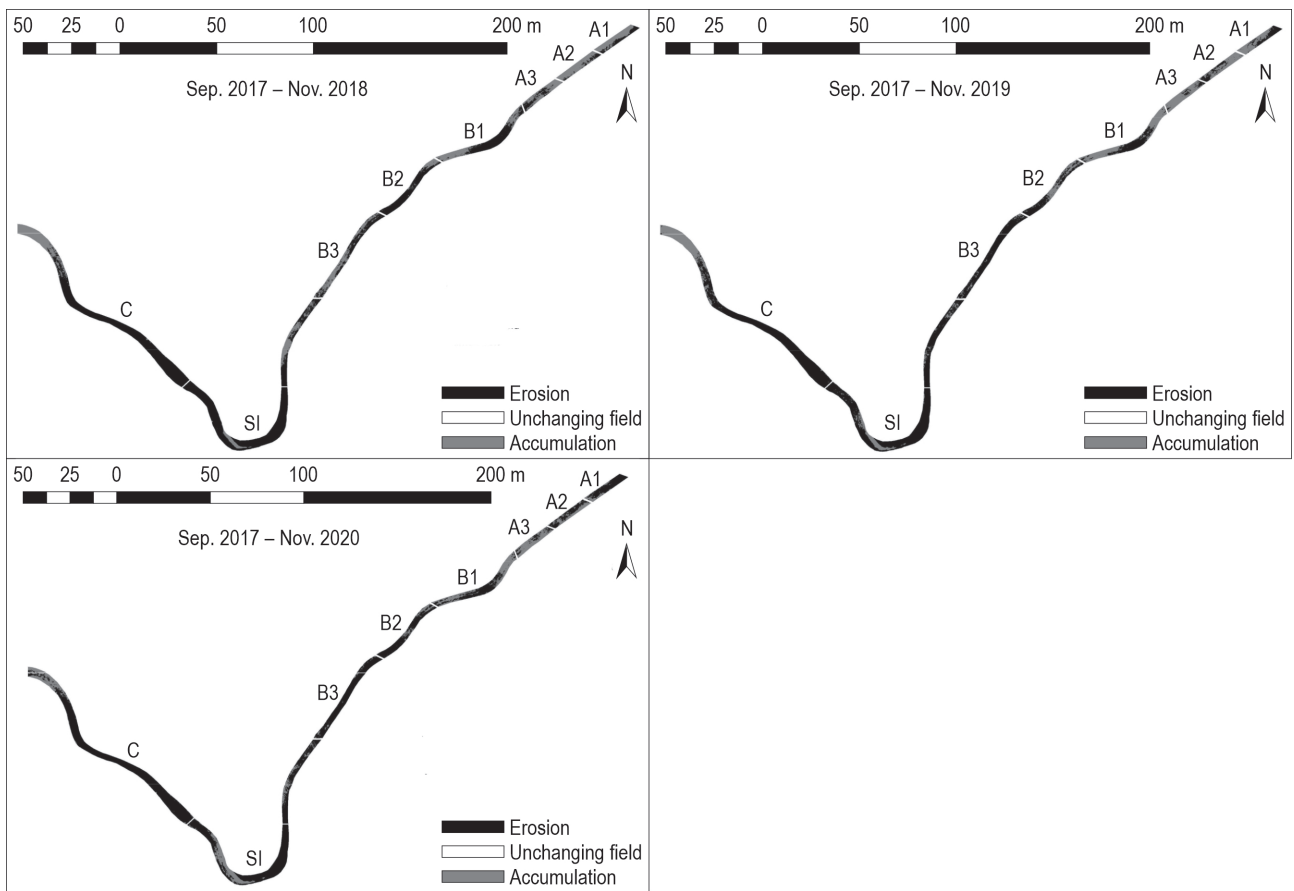
Fig. 7 Map of volume (m³) deteriorations of the first, second, and third year

according to the results of the analyses made by taking September 2017 as a constant. In addition, Fig. 7 presents the first-, second-, and third-year volumetric deterioration maps in the blocks. When Table 2 is examined, it can be seen that the dynamic movement of erosion and accumulation in all blocks was found to continue in the three-years time series. It was determined that this mobility was greater in the control block (C) than in the blocks with 25 m (A1, A2, and A3) and 50 m (B1, B2 and B3) open-top culverts.

The volume of erosion and accumulation per square meter, which is important in the comparison of deteriorations in the blocks, was also found. Table 3 presents the erosion and accumulation volume per square meter of the blocks by including the sum of A parcels (AS) and the sum of B parcels (BS). In addition, the data graphs for the first-, second-, and third-year are given in Fig. 8. When Table 3 is examined, it can be seen that there was 4.9 times more erosion in the control block (C) compared to the AS average and 1.98 times more erosion according to the BS average. These results revealed the effectiveness of open-top culverts.

Furthermore, when Table 3 is examined, it can be seen that there was a 1.71-fold accumulation in the control block (C) compared to the AS average and a 6-fold accumulation in the BS average. On the road surface, minimum erosion was calculated at A2, A3, and B1 (0.000 m³ m⁻²), maximum erosion at B3 (0.211 m³ m⁻²), minimum accumulation at A1, A2, and B1 (0.000 m³ m⁻²) and maximum accumulation at A3 (0.064 m³ m⁻²). These results and the average results show the dynamic mobility of the blocks. Due to the location of the A1 parcel, a surface flow has occurred from outside the work area towards this parcel. For this reason, in the first two years, the volume of accumulation in the A1 parcel was high (Fig. 8), due to external factors (Fig. 9). This is a natural process, and parcel A1 is included in the results.

In addition to the volumetric deterioration related to the blocks, areal deterioration was detected in the study. Likewise, as a result of the analyses made by taking the blocks cleared of external factors in September 2017, as a fixed, three-years time series, the areal erosion and accumulation sizes of each block are

Table 3 Volumetric erosion and accumulation from DEM differences per square meter on blocks

DEM difference between flights	Volumetric erosion (−) and accumulation (+) per square meter on blocks, m³ m⁻²																	
	A1		A2		A3		AS		B1		B2		B3		BS		C	
	(−)	(+)	(−)	(+)	(−)	(+)	(−)	(+)	(−)	(+)	(−)	(+)	(−)	(+)	(−)	(+)	(−)	(+)
Sep. 2017 – Nov. 2017	0.056	0.000	0.003	0.009	0.000	0.013	0.022	0.007	0.030	0.000	0.057	0.001	0.026	0.000	0.034	0.000	0.104	0.017
Sep. 2017 – Apr. 2018	0.072	0.003	0.013	0.007	0.001	0.047	0.031	0.018	0.006	0.026	0.058	0.002	0.110	0.000	0.062	0.009	0.067	0.029
Sep. 2017 – Nov. 2018	0.009	0.030	0.000	0.000	0.002	0.021	0.004	0.050	0.020	0.010	0.074	0.001	0.013	0.009	0.030	0.007	0.122	0.021
Sep. 2017 – Mar. 2019	0.032	0.001	0.004	0.007	0.000	0.047	0.013	0.017	0.000	0.040	0.018	0.009	0.046	0.000	0.024	0.015	0.084	0.032
Sep. 2017 – Apr. 2019	0.020	0.001	0.001	0.015	0.000	0.058	0.008	0.023	0.003	0.012	0.035	0.005	0.078	0.000	0.043	0.005	0.100	0.024
Sep. 2017 – May 2019	0.021	0.001	0.001	0.017	0.000	0.046	0.040	0.020	0.003	0.015	0.044	0.003	0.101	0.000	0.056	0.005	0.110	0.025
Sep. 2017 – June 2019	0.021	0.000	0.003	0.022	0.000	0.064	0.009	0.027	0.006	0.005	0.034	0.004	0.102	0.000	0.054	0.003	0.114	0.058
Sep. 2017 – July 2019	0.034	0.000	0.017	0.003	0.002	0.016	0.019	0.006	0.001	0.014	0.079	0.000	0.084	0.000	0.055	0.005	0.070	0.020
Sep. 2017 – Aug. 2019	0.051	0.000	0.022	0.003	0.006	0.008	0.028	0.003	0.001	0.011	0.044	0.005	0.110	0.000	0.059	0.005	0.077	0.016
Sep. 2017 – Sep. 2019	0.013	0.002	0.010	0.004	0.001	0.013	0.008	0.006	0.006	0.006	0.045	0.007	0.073	0.000	0.044	0.004	0.108	0.026
Sep. 2017 – Nov. 2019	0.020	0.030	0.007	0.028	0.002	0.026	0.010	0.028	0.008	0.013	0.023	0.011	0.052	0.000	0.031	0.007	0.084	0.024
Sep. 2017 – Apr. 2020	0.026	0.002	0.011	0.006	0.010	0.010	0.016	0.006	0.007	0.014	0.038	0.011	0.065	0.002	0.040	0.008	0.104	0.021
Sep. 2017 – May 2020	0.030	0.000	0.021	0.000	0.002	0.009	0.018	0.003	0.011	0.001	0.060	0.001	0.074	0.000	0.050	0.001	0.091	0.017
Sep. 2017 – June 2020	0.053	0.000	0.010	0.003	0.001	0.021	0.023	0.007	0.009	0.007	0.042	0.004	0.130	0.000	0.070	0.003	0.054	0.051
Sep. 2017 – July 2020	0.130	0.001	0.004	0.014	0.001	0.013	0.049	0.009	0.027	0.000	0.054	0.001	0.047	0.000	0.042	0.000	0.131	0.001
Sep. 2017 – Aug 2020	0.060	0.000	0.028	0.001	0.006	0.002	0.033	0.001	0.044	0.000	0.178	0.000	0.211	0.000	0.148	0.000	0.199	0.001
Sep. 2017 – Sep. 2020	0.086	0.000	0.026	0.001	0.001	0.011	0.041	0.004	0.017	0.001	0.054	0.002	0.087	0.000	0.056	0.001	0.115	0.013
Sep. 2017 – Oct. 2020	0.048	0.003	0.002	0.016	0.000	0.061	0.019	0.025	0.007	0.009	0.048	0.003	0.078	0.000	0.048	0.004	0.103	0.019
Sep. 2017 – Nov. 2020	0.034	0.000	0.008	0.003	0.002	0.009	0.016	0.004	0.008	0.003	0.055	0.001	0.063	0.000	0.043	0.001	0.119	0.005
Average	0.043	0.005	0.010	0.013	0.007	0.026	0.021	0.014	0.011	0.010	0.055	0.004	0.082	0.001	0.052	0.004	0.103	0.024
Minimum	0.009	0.000	0.000	0.000	0.000	0.002	0.004	0.001	0.000	0.000	0.018	0.004	0.013	0.001	0.024	0.004	0.054	0.024
Maximum	0.130	0.030	0.028	0.028	0.010	0.064	0.049	0.050	0.044	0.040	0.178	0.011	0.211	0.009	0.148	0.015	0.188	0.058

Table 4 Areal erosion and accumulation from DEM differences on blocks

| DEM difference between flights by year	Areal erosion (−) and accumulation (+) on blocks, m²													
	A1		A2		A3		B1		B2		B3		C3	
	(−)	(+)	(−)	(+)	(−)	(+)	(−)	(+)	(−)	(+)	(−)	(+)	(−)	(+)
First Year Sep. 2017 – Nov. 2018	9.992	47.312	0.027	53.778	2.006	18.266	37.510	21.013	67.733	1.507	31.813	23.642	343.57	84.02
Second Year Sep. 2017 – Nov. 2019	19.860	30.628	8.257	24.696	1.811	27.123	15.334	28.106	28.930	12.577	104.34	0.671	311.50	101.24
Third Year Sep. 2017 – Nov. 2020	34.079	0.754	9.765	4.039	2.012	10.062	17.066	7.733	57.324	1.743	131.17	0.695	375.58	23.82
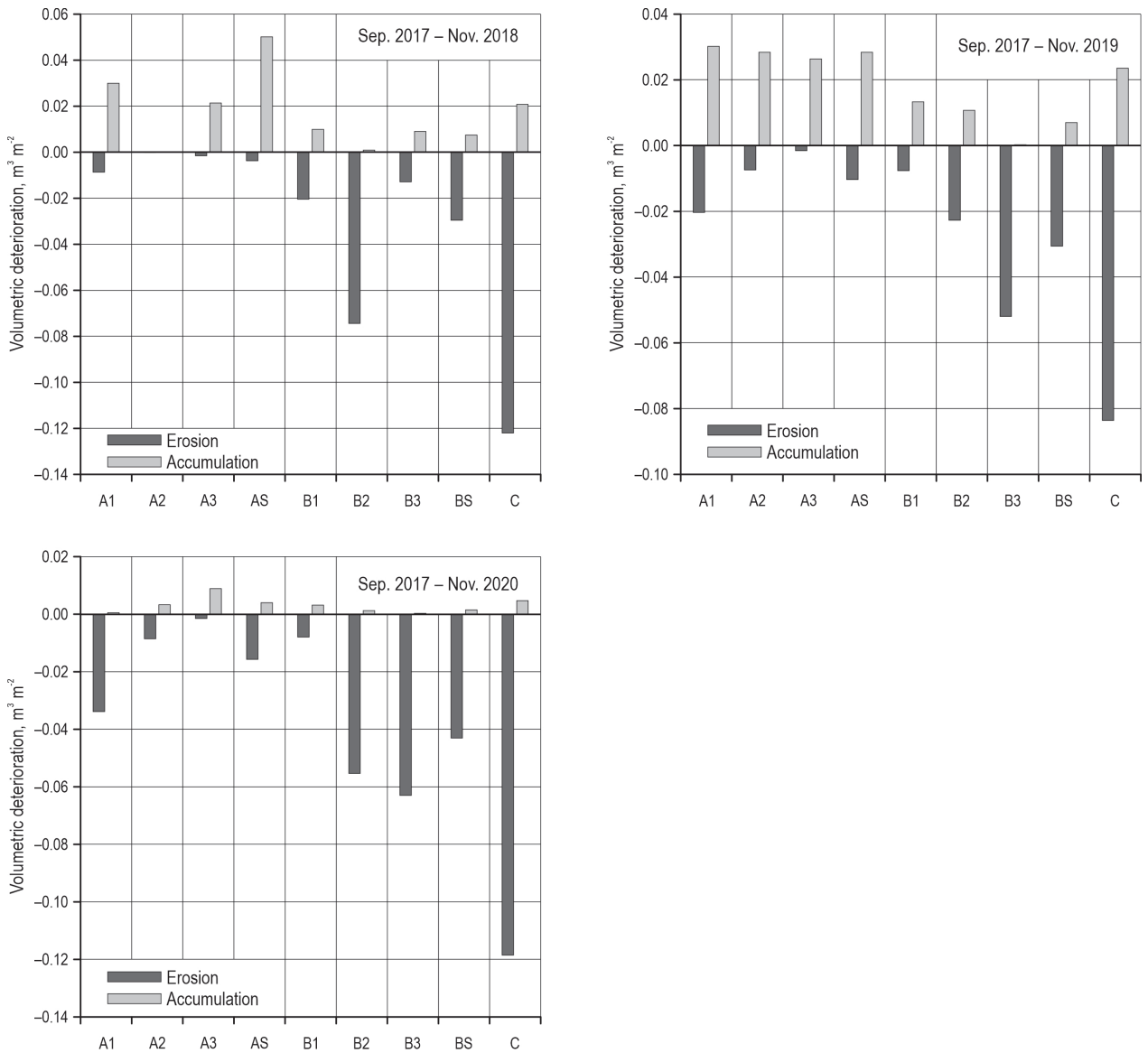
Fig. 8 Volumetric erosion and accumulation graph per square meter on blocks for the first-, second-, and third-year blocks
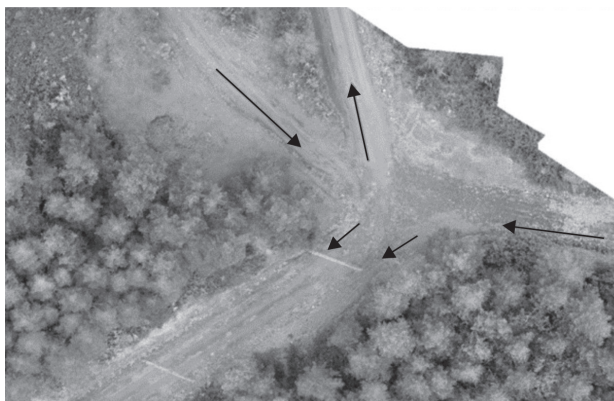

Fig. 9 Water and sediment from outside the study area of parcel A1

presented in Table 4. In addition, Fig. 10 presents the first-, second-, and third-year areal deterioration maps in the blocks.

When Table 4 is examined, it can be seen that the dynamic movement of erosion and deposition in all blocks was found to continue in the time series. It was determined that this mobility was greater in the control block (C) than in the blocks with 25 m (A1, A2, and A3) and 50 m (B1, B2, and B3) open-top culverts.

In the study, in addition to the volumetric erosion and accumulation volume per square meter in the blocks, the areal erosion and accumulation sizes per square meter in the blocks were also determined. Table 5 presents areal erosion and areal accumulation per
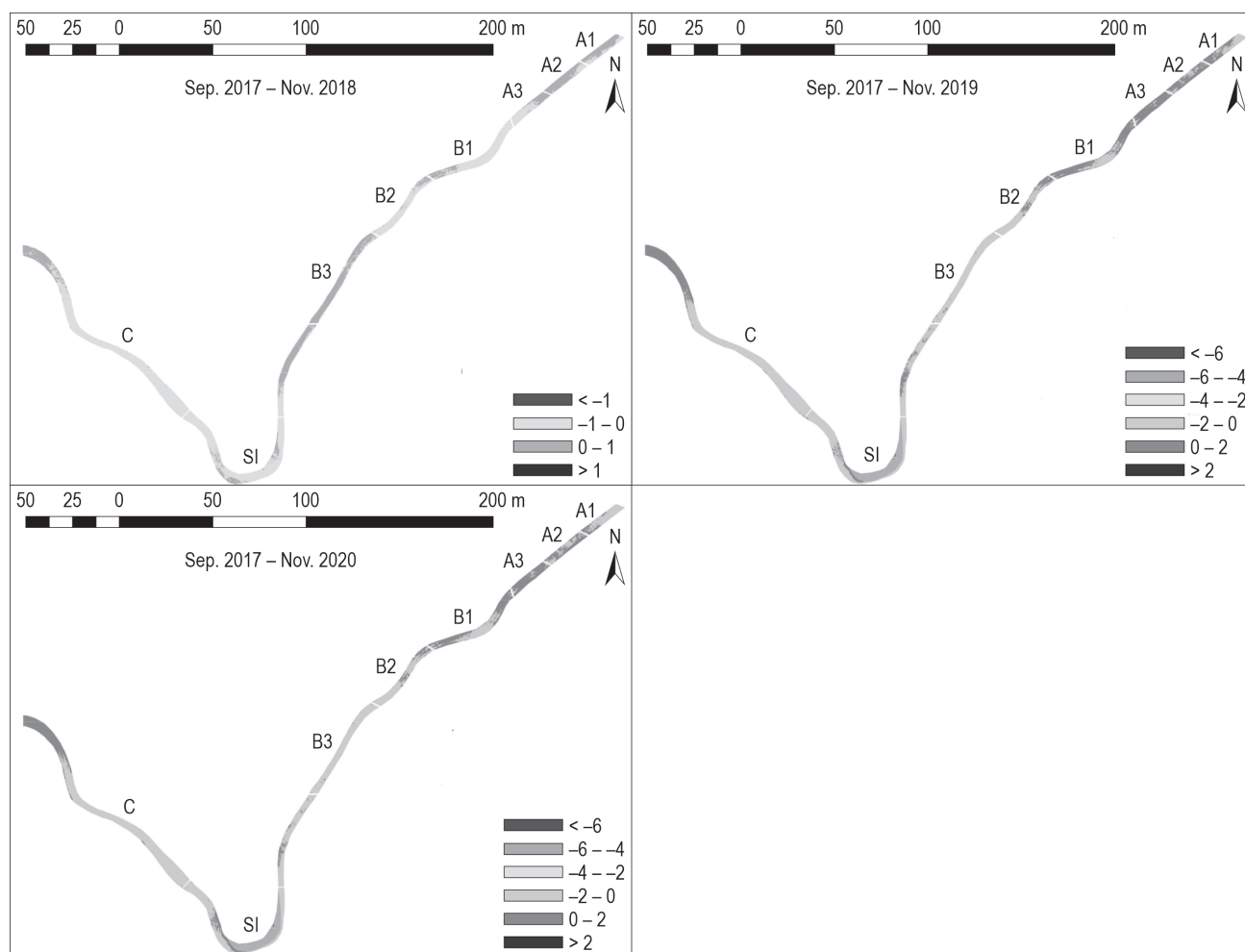
Fig. 10 Map of first-, second-, and third-year areal (m^2) deteriorations

square meter in the blocks by including the sum of A blocks (AS) and the sum of B blocks (BS). In addition, the data graphs for the first-, second-, and third-year are given in Fig. 11. When Table 5 and graphs are examined, it can be seen that, in terms of areal, the erosion was 3.3 times higher in the control block (C) compared to the AS average and 1.4 times compared to the BS average. These results revealed the effectiveness of open-top culverts. In addition, it can be seen that there was a 1.11-fold accumulation in the control block (C) compared to the AS average and a 2.92 accumulation compared to the BS average. On the road surface, minimum erosion was calculated at A2 and A3 (0.000 m^2), maximum erosion at B2 (0.983 m^2), minimum accumulation at A1, B1, and B3 (0.000 m^2), maximum accumulation at A3 (0.739 m^2). Deteriorations were clearly seen in the images (before and after) taken from the control block in the study area (Fig. 12).

However, although the erosion or accumulation are in the blocks, accumulations such as sediment, leaves, etc. have occurred, especially in the open-top culverts, and for this reason, on the days of the flights, the open-top culverts were checked and those with accumulations were cleaned. In addition, the ferrous iron bands, which had loosened due to heavy vehicles, were fixed again. It shoukld also be noted that erosion from transport moves away from the road surface towards the edge ditches.

3.2 Findings of Statistical Analysis

According to the results of the analysis of variance (Table 6), carried out to find out whether there is a difference between the blocks in terms of the volumetric deterioration per square meter, it was determined that there was a statistically significant difference between the volumetric erosion in the blocks ($p < 0.05$). The greatest

Table 5 Areal erosion and accumulation from DEM differences per square meter on blocks

DEM difference between flights	Areal erosion (–) and accumulation (+) per square meter on blocks, m²																	
	A1		A2		A3		AS		B1		B2		B3		BS		C	
	(–)	(+)	(–)	(+)	(–)	(+)	(–)	(+)	(–)	(+)	(–)	(+)	(–)	(+)	(–)	(+)	(–)	(+)
Sep. 2017 – Nov. 2017	0.494	0.000	0.039	0.136	0.004	0.208	0.196	0.108	0.367	0.004	0.590	0.010	0.335	0.004	0.405	0.005	0.673	0.193
Sep. 2017 – Apr. 2018	0.631	0.047	0.175	0.094	0.009	0.514	0.292	0.206	0.086	0.331	0.542	0.032	0.922	0.000	0.548	0.120	0.512	0.235
Sep. 2017 – Nov. 2018	0.103	0487	0.000	0.633	0.025	0.224	0.046	0.453	0.256	0.143	0.660	0.015	0.163	0.121	0.309	0.104	0.668	0.163
Sep. 2017 – Mar. 2019	0.291	0.019	0.057	0.105	0.002	0.616	0.126	0.231	0.005	0.508	0.228	0.119	0.535	0.006	0.289	0.198	0.617	0.269
Sep. 2017 – Apr. 2019	0.207	0.012	0.022	0.219	0.000	0.739	0.083	0.303	0.049	0.187	0.404	0.061	0.798	0.001	0.459	0.076	0.644	0.226
Sep. 2017 – May 2019	0.224	0.010	0.022	0.247	0.000	0.617	0.089	0.274	0.045	0.222	0.095	0.037	0.915	0.000	0.438	0.082	0.657	0.223
Sep. 2017 – June 2019	0.227	0.006	0.042	0.271	0.000	0.678	0.097	0.299	0.078	0.086	0.402	0.052	0.926	0.000	0.525	0.040	0.661	0.271
Sep. 2017 – July 2019	0.368	0.004	0.222	0.026	0.033	0.176	0.217	0.064	0.012	0.229	0.679	0.004	0.814	0.000	0.518	0.077	0.602	0.193
Sep. 2017 – Aug. 2019	0.502	0.002	0.289	0.036	0.080	0.087	0.303	0.039	0.021	0.179	0.448	0.065	0.952	0.000	0.528	0.074	0.642	0.167
Sep. 2017 – Sep. 2019	0.175	0.032	0.134	0.057	0.014	0.166	0.112	0.081	0.077	0.102	0.491	0.080	0.698	0.004	0.445	0.054	0.614	0.252
Sep. 2017 – Nov. 2019	0.204	0.315	0.097	0.291	0.022	0.333	0.114	0.313	0.105	0.192	0.282	0.123	0.535	0.003	0.335	0.093	0.606	0.197
Sep. 2017 – Apr. 2020	0.300	0.029	0.146	0.080	0.126	0.142	0.197	0.080	0.091	0.198	0.403	0.143	0.680	0.022	0.421	0.108	0.663	0.206
Sep. 2017 – May 2020	0.321	0.000	0.268	0.007	0.027	0.128	0.213	0.042	0.157	0.018	0.615	0.016	0.741	0.002	0.519	0.010	0.656	0.188
Sep. 2017 – June 2020	0.517	0.001	0.139	0.034	0.016	0.299	0.241	0.104	0.120	0.115	0.465	0.057	0.979	0.001	0.576	0.051	0.488	0.319
Sep. 2017 – July 2020	0.810	0.010	0.053	0.194	0.022	0.189	0.322	0.125	0.339	0.005	0.562	0.014	0.518	0.005	0.469	0.007	0.841	0.012
Sep. 2017 – Aug 2020	0.635	0.001	0.366	0.013	0.091	0.031	0.381	0.014	0.508	0.000	0.983	0.002	0.996	0.001	0.832	0.001	0.914	0.007
Sep. 2017 – Sep. 2020	0.783	0.000	0.340	0.019	0.022	0.162	0.405	0.056	0.219	0.015	0.562	0.024	0.813	0.001	0.559	0.011	0.696	0.142
Sep. 2017 – Oct. 2020	0.438	0.046	0.031	0.212	0.000	0.727	0.172	0.310	0.105	0.137	0.512	0.035	0.778	0.001	0.494	0.054	0.666	0.189
Sep. 2017 – Nov. 2020	0.351	0.008	0.115	0.048	0.025	0.124	0.174	0.056	0.116	0.053	0.559	0.017	0.673	0.004	0.463	0.023	0.730	0.046
Average	0.399	0.054	0.135	0.143	0.027	0.324	0.199	0.166	0.145	0.143	0.499	0.048	0.725	0.009	0.481	0.063	0.661	0.184
Minimum	0.103	0.000	0.000	0.007	0.000	0.031	0.046	0.014	0.005	0.000	0.095	0.002	0.163	0.000	0.289	0.001	0.488	0.007
Maximum	0.810	0.487	0.366	0.633	0.126	0.739	0.405	0.453	0.508	0.508	0.983	0.143	0.996	0.121	0.832	0.198	0.914	0.319

Table 6 Results of analysis of variance regarding deteriorations in blocks

Parameters	Blocks	Number of samples	Mean	Standard error	p*
Volumetric erosion m³ m⁻²	AS	19	0.140a	0.003	0.000
	BS	19	0.223b	0.006	
	C	19	0.318c	0.007	
Areal erosion m²	AS	19	0.199a	0.024	0.000
	BS	19	0.481b	0.027	
	C	19	0.661c	0.022	
Z difference m	AV	19	0.336a	0.046	0.000
	BV	19	0.180b	0.018	
	C	19	0.058c	0.016	

AV = Z difference average of A block
BV = Z difference average of B block
* p < 0.05

volumetric erosion was found in the control block (C) (0.318 m³m⁻²), the lowest in the sum of blocks A (0.140 m³ m⁻²) and between both blocks in the sum of blocks B (0.223 m³ m⁻²). The situation was similar for the size of the erosion. It was determined that there was a statistically significant difference between the areal size of erosion in the blocks ($p<0.05$). The maximum areal size of erosion was found In the control block (C) (0.661 m²), the lowest in the sum of blocks A (0.199 m²), and in the sum of blocks B between both blocks (0.481 m²). However, there was no statistically significant difference in other volumetric and areal accumulation data ($p>0.05$). In addition, according to the results of the normalized Z differences in the blocks, it was determined that there was a statistically significant difference between the Z differences in the blocks ($p<0.05$). Each block was placed in different groups.
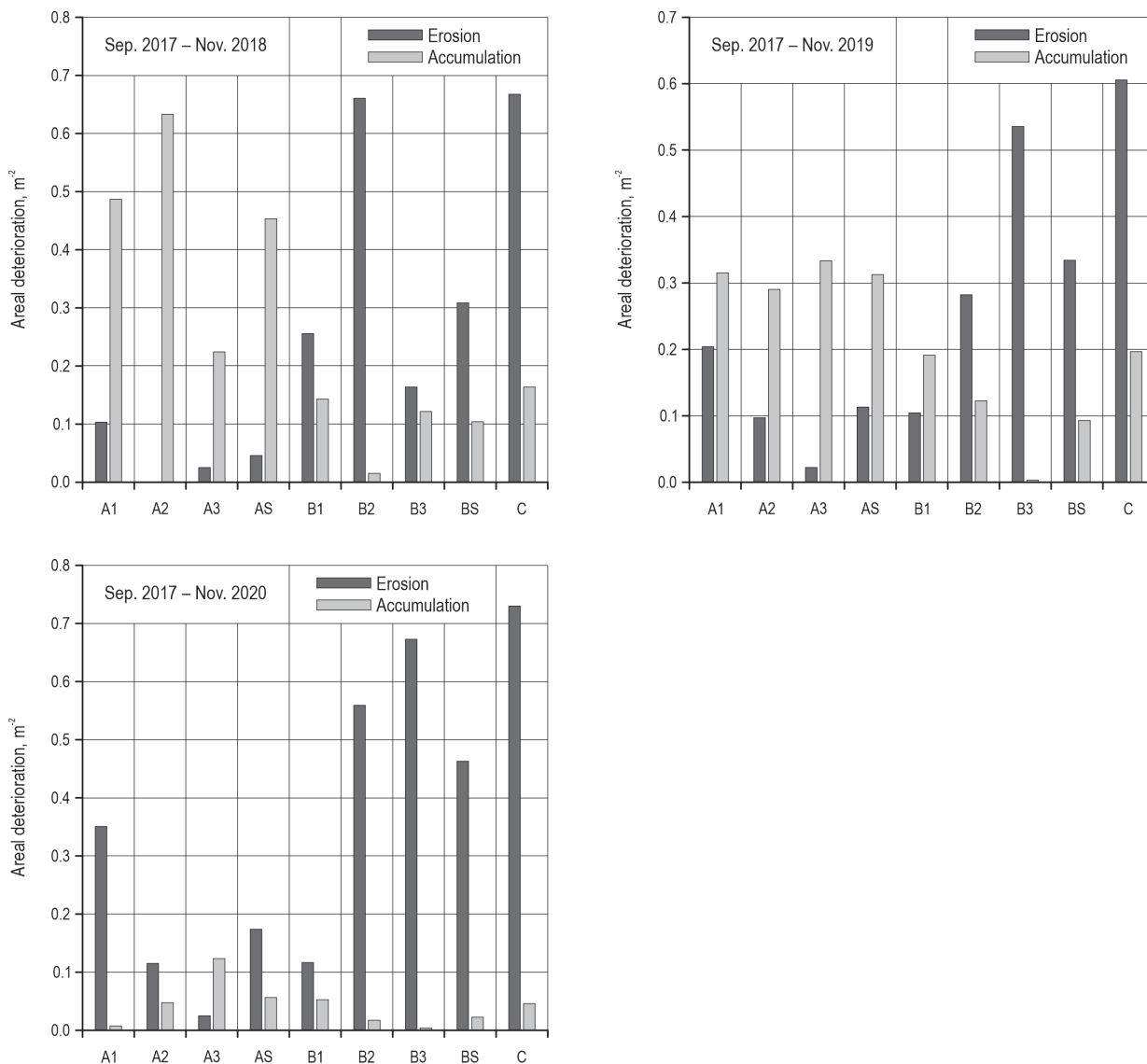
Fig. 11 Graph of areal (m²) erosion and accumulation per square meter on blocks for the first-, second-, and third-year

Fig. 12 Deterioration images on the control block taken in the field

4. Discussion

In the study, the effectiveness of wooden open-top culverts in protecting against deterioration of the forest road surface was examined by using UAVs. Although there is a limited use of the UAV system in road-related studies, so far, there has been no study on the effectiveness of the more specific open-top culverts in the literature. The open-top culverts used in the study are used to remove the damaging waters from the road surface in the fastest way by flowing along the road axis on forest roads (Bayoğlu 1997, Erdaş 1997, Anonymous 2018).

Remote sensing techniques are used for various monitoring purposes, both in planning and projecting and after road construction on forest roads. One of the important issues studied on forest roads is monitoring road surface deterioration. There are no studies in the literature on the monitoring of deterioration of the road surface for protection (hydraulic architectural, etc.). The studies are concerned with monitoring the natural state of the unprotected road (such as the control block in our study).

In other studies, as well as in our study, it was stated that volumetric and areal deteriorations of the road surface differed temporally (Akgul et al. 2017, Akay et al. 2018, Türk et al. 2022b). In their study, Akgul et al. (2017) and Akay et al. (2018) examined the deterioration in the road surface with a terrestrial laser scanner for a year (in three-month periods). Türk et al. (2022b) investigated forest road surface degradation with a UAV for about 14 months. In another study, Eker (2023) used PPK-integrated close-range terrestrial photogrammetry (CRTP) with handheld mobile laser scanning (HMLS) called TORCH that uses the SLAM algorithm to measure and compare forest road surface deterioration. When we compared these four studies with ours, similar results were found. It is understood from the studies that the dynamic mobility of erosion and accumulation continues periodically.

Akay et al. (2018) found the average monthly areal erosion for the 100-meter-long forest road (longitudinal gradient: 6%, material of the running surface: sediment) to be 49.6 m^2 and the accumulation to be 58.6 m^2. In addition, the average monthly volumetric erosion was –0.75 m^3, and the accumulation was 0.51 m^3. However, according to the data from September 2017 – November 2020 (37 months) in our study, for 100 m, the average monthly areal and volumetric deterioration values in the control block (areal erosion 3.34 m^2, accumulation 0.93 m^2, volumetric erosion –0.51 m^3, volumetric accumulation 0.11 m^3) were smaller. This difference may be due to the fact that

dynamic mobility continues throughout the study and the photogrammetric methods used (terrestrial laser scanners and UAVs).

According to Ciobanu et al. (2012), as a result of the remote transportation work carried out by trucks on 2 km of secondary forest roads (longitudinal gradient: 9%, material of the running surface: sediment) in the 10-day study carried out by the traditional method, the road surface deterioration was calculated as follows: a total areal erosion of –23.02 m^2 (–2.302 m^2/day) and volumetric erosion of –8.96 m^3 (–0.896 m^3/day). In our study, the average daily areal erosion (2.22 m^2/day) is similar in the control block for 2 km, while there is a significant difference in volumetric erosion (–0.34 m^3/day). In another study, Săceanu (2013) made a road comparison using the traditional method after remote transportation work with trucks was carried out on 2.5 km of forest roads (material of the running surface: sediment) over an 8-month period. As a result, areal erosion of a total of 224.2 m^2 (average 28.02 m^2/month –0.94 m^2/day) was detected on the road surface. In our study, 2.78 m^2/day areal erosion was found for the 2.5 km control block (as a result of the rate of the block length). It is thought that the reason for these differences may be the difference in the frequency of use of the roads, the tonnage of loaded vehicles, transport season, technical features of the road, methods, etc.

Apart from the effectiveness of open-top culverts, the other aim of our study is to map the deterioration of the road surface using UAVs. Similar to our study, Akgul et al. (2017) and Akay et al. (2018) mapped road surface deterioration based on terrestrial laser scanners, while Türk et al. (2022b) and Dobson et al. (2013) mapped road surface deterioration based on UAV results.

Other studies are related to the use of UAV systems in surface change (earthwork, excavation, filling calculations, etc.). In these studies, it is emphasized that the UAV data results are highly overlapping with the ground measurement results, and that UAV systems can be used in such studies (Hrůza et al. 2016, Yurtseven et al. 2019, Ciritcioğlu and Buğday 2022, Kınalı and Çalışkan 2022, Hasegawa et al. 2023). In our study, the accuracy of the UAV data results was found to be high by utilizing buckets with known volume and height.

5. Conclusions

In this study, to evaluate the effectiveness of open-top culverts on road surface deterioration within the study scope, the average Z-value differences of pixels in the blocks and DEM differences determined by vector

data were used. The findings indicated that open-top culverts were effective in mitigating deterioration. For about three years (September 2017 – November 2020), it was found that the dynamic movement of erosion and accumulation in all blocks continued in the time series. This mobility was determined more in the control block than in the blocks where there were open-top culverts installed at intervals of 25 m and 50 m. These results revealed the effectiveness of open-top culverts, and it was determined that the open-top culverts with a 25 m interval were more effective than those with a 50 m interval. In practice, 25 m interval open-top culverts should be used.

In general, the eroded material in the study area is carried to the edge of ditches. Furthermore, although erosion or accumulation occurred within the blocks, sediment, leaves, etc. were accumulated, especially inside the open-top culverts. For this reason, open-top culverts should be periodically checked and maintained. Although the conditions change depending on rain precipitation, the open-top culverts should be cleaned every 2 months. In addition, the flat ferrous bands that have been loosened by heavy tonnage vehicles should be fixed again.

It has been observed in the Z values graph that the deterioration in the mean Z values of the blocks is progressing with relatively lower changes, especially when compared with the control block. A1, A2, and A3 parcels showed similar changes in the range of ±20 cm when compared to B1, B2, and B3 parcels, while the mean Z changes were higher in the control block. This study reveals the need to evaluate the effects of open-top culverts by using them in an environment where external factors can be kept under control, i.e. under laboratory conditions. In addition, it is thought that this study should be carried out in laboratory conditions in order to determine effectively the deployment intervals of open-top culverts on different slopes and intervals.

According to the results of the analysis of variance carried out to find out whether there is a difference in the volumetric deterioration per square meter between the blocks, it was determined that there was a statistically significant difference between the volumetric erosion in the blocks ($p < 0.05$). The volumetric erosion was found to be the highest (0.318 $m^3 m^{-2}$) in the control block, the lowest (0.140 $m^3 m^{-2}$) in the AS blocks and between the two blocks in the BS blocks (0.223 $m^3 m^{-2}$). A similar situation was found in the areal erosion. These statistical results prove the use of 25 m interval open-top culverts in practice.

In the study, in addition to the volumetric deteriorations related to the blocks, areal deteriorations were also detected. It has been concluded that UAV systems can be used to map road surface deterioration. In addition, it was concluded that it would be better for these methods to receive data every 3 months rather than monthly. In determining the volumetric deterioration obtained with traditional methods, the experience of the personnel performing measurement of the land gains importance. The values obtained are time-consuming and there may be variability in the measurement results. In this study, the deterioration of the road surface has been detected with a UAV, which is one of the automatic methods, so the errors of the traditional measurement methods have been prevented.

In this study, high-resolution orthophoto maps were produced with a UAV and the results were determined in a way that can reduce the cost of road maintenance and repair work by applying this costly work only to the deteriorated local areas instead of the entire road. To conclude, the UAV system can be effectively used in the monitoring and evaluation of the road surface.

Acknowledgments

6. References

AASHTO, 2001: AASHTO Guidelines for Geometric Design of Very Low-Volume Local Roads (ADT ≤ 400), 1st Edition. American Association of State Highway and Transportation Officials, Washington, D.C.

Abhijit, P., Jalindar, P., 2011: Effects of bad drainage on roads. Civ. Environ. Res. 1(1): 1–7.

Adlinge, S.S., Gupta, A.K., 2013: Pavement deterioration and its causes. International Journal of Innovative Research and Development 2(4): 437–450.

Akay, A.O., Akgul, M., Demir, M., 2018: Determination of temporal changes on forest road pavement with terrestrial laser scanner. Fresenius Environmental Bulletin 27(3): 1437–1448.

Akgul, M., Yurtseven, H., Akburak, S., Demir, M., Cigizoglu, M.H.K., Ozturk, T., Eksi, M., Akay, A.O., 2017: Short term monitoring of forest road pavement degradation using terrestrial laser scanning. Measurement 103: 283–293. https://doi.org/10.1016/j.measurement.2017.02.045

Akgul, M., Akburak, S., Yurtseven, H., Akay, A.O., Cigizoglu, H.K., Demir, M., Ozturk, T., Eksi, M., 2019: Potential impacts of weather and traffic conditions on road surface performance in terms of forest operations continuity. Applied Ecology and Environmental Research 17(2): 2533–2550. http://dx.doi.org/10.15666/aeer/1702_2533255

Anon., 2018: Portland Water District, http://www.pwd.org/news/publications.php. (accessed 13.03.2018).

Attoh-Okine, N., Offei, A., 2013: Pavement condition surveys–overview of current practices. Delaware Center for Transportation, University of Delaware: Newark, DE, USA.

Bayoğlu, S., 1997: Forest Transport Facilities and Vehicles. İstanbul University Faculty of Forestry Press: İstanbul, 434 p.

BCMF, 2018: B.C. Forest road engineering guidebook. For. Prac. Br., B.C. Min. For., Victoria, B.C. Forest Practices Code of British Columbia Guidebook. http://www.for.gov.bc.ca/tasb/legsregs/fpc/fpcguide/guidetoc.htm. 2002 (accessed 20 March 2018).

Biçici, S., Zeybek, M., 2021: Effectiveness of training sample and features for random forest on road extraction from unmanned aerial vehicle-based point cloud. Transportation Research Record 2675(12): 401–418. https://doi.org/10.1177/03611981211029645

Boghian, V., Apăfăian, A., Bratu, C., Ignea, G., 2015: A review on degradation factors affecting the forest roads and their prevention. Proceedings of the Biennial International Symposium. Forest and sustainable development, Brașov, Romania, 24–25th October 2014. Transilvania University Press.

Buğday, E., 2018: Capabilities of using UAVs in forest road construction activities. European Journal of Forest Engineering 4(2): 56–62. https://doi.org/10.33904/ejfe.499784

Chang, K.T.J., Chang, R., Liu, J.K., 2005: Detection of pavement distresses using 3D laser scanning technology. Computing in Civil Engineering 1–11 p. https://doi.org/10.1061/40794(179)103

Cheng, B., Ji, H., Wang, Y., 2023: A new method for constructing roads map in forest area using UAV images. Journal of Computational Methods in Sciences and Engineering 23(2): 573–587.

Ciobanu, V., Alexandru, V., Saceanu, S., 2012: Degradation forms of forest gravel road roadways under heavy vehicles used in timber transport. Bulletin of the Transilvania University of Brasov. Series II: Forestry• Wood Industry• Agricultural Food Engineering (2012): 37–42.

Ciritcioğlu, M.G., Buğday, E., 2022: Assessment of Unmanned Aerial Vehicle use opportunities in forest road project (Düzce Sample). Journal of Bartın Faculty of Forestry 24(2): 247–257. https://doi.org/10.24011/barofd.1066636

Díaz-Vilariño, L., González-Jorge, H., Martínez-Sánchez, J., Bueno, M., Arias, P., 2016: Determining the limits of unmanned aerial photogrammetry for the evaluation of road runoff. Measurement 85: 132–141. https://doi.org/10.1016/j.measurement.2016.02.030

Dobson, R.J., Brooks, C., Roussi, C., Colling, T., 2013: Developing an unpaved road assessment system for practical deployment with high-resolution optical data collection using a helicopter UAV. In International Conference on Unmanned Aircraft Systems (ICUAS), 235–243 p.

Eker, R., 2023: Comparative use of PPK-integrated close-range terrestrial photogrammetry and a handheld mobile laser scanner in the measurement of forest road surface deformation. Measurement 206: 112322. https://doi.org/10.1016/j.measurement.2022.112322

Erdaş, O., 1997: Forest roads, Karadeniz Technical University Press: Trabzon, 298 p.

Fwa, T.F., 2005: The handbook of highway engineering. CRC press

George, K.P., Rajagopal, A.S., Lim, L.K., 1989: Models for predicting pavement deterioration, Transp. Res. Rec. 1215: 1–7.

GDF, 2008: Forest roads planning, construction and maintenance. Report no. 292, Ankara.

GDF, 2011: Kardüz Forest Management Department Functional Forest Management Plan, Gölyaka Forest Management Directorate.

Grajewski, S.M., 2023: Evaluation of light falling weight deflectometer for in situ measurement of secondary deformation modulus of various forest road pavements. Croatian Journal of Forest Engineering 44(2): 313–326. https://doi.org/10.5552/crojfe.2023.2125

Gülci, S., Kılınç, G., 2018: Assessment of drone-assisted soil stockpile volume measurement. In Proceedings of International Academıc Research Congress, 1108–1812 p.

Gülci, S., Şireli, S., 2019: The evaluation of SfM technique in the determination of surface deformation on skidding roads following timber harvesting. European Journal of Forest Engineering 5(2): 52–60. https://doi.org/10.33904/ejfe.600860

Haas, R., 2001: Reinventing the (pavement management) wheel. – Proceedings of the Fifth International Conference on Managing Pavements, August 11–14, Seattle, Washington.

Hasegawa, H., Sujaswara, A.A., Kanemoto, T., Tsubota, K., 2023: Possibilities of Using UAV for Estimating Earthwork Volumes during Process of Repairing a Small-Scale Forest Road, Case Study from Kyoto Prefecture, Japan. Forests 14(4): 677. https://doi.org/10.3390/f14040677

Herr, B., 2001: Calibration and operation of pavement profile scanners. RPUG, Lake Tahoe.

Herr, B., 2009: PSI Current Technology Overview, white paper. July 11 2009.

Hrůza, P., Mikita, T., Janata, P., 2016: Monitoring of forest hauling roads wearing course damage using unmanned aerial systems. Acta Universitatis Agriculturae et Silviculturae Mendelianae Brunensis 64(5): 1537–1546. http://dx.doi.org/10.11118/actaun201664051537

Huang, Y., Copenhaver, T., Hempel, P., 2011: Texas Department of Transportation 3D transverse profiling system for high-speed rut measurement. Journal of Infrastructure Systems 19(2): 221–230. https://doi.org/10.1061/(ASCE)IS.1943-555X.0000088

Kınalı, M., Çalışkan, E., 2022: Use of Unmanned Aerial Vehicles in Forest Road Projects. Journal of Bartın Faculty of Forestry 24(3): 530–541. https://doi.org/10.24011/barofd.1073229

Kramer, B.W., 2001: Forest road contracting, construction, and maintenance for small forest woodland owners. Oregon State University 35: 65–73.

Kaare, K.K., Kristjan, K., Ott, K., 2012: Tire and pavement wear interaction monitoring for road performance indicators. Estonian Journal of Engineering 18(4): 324–335. http://dx.doi.org/10.3176/eng.2012.4.04

Kusak, L., Unel, F.B., Alptekin, A., Celik, M.O., Yakar, M., 2021: Apriori association rule and K-means clustering algorithms for interpretation of pre-event landslide areas and landslide inventory mapping. Open Geosciences 13(1): 1226–1244. https://doi.org/10.1515/geo-2020-0299

Li, Q., Yao, M., Yao, X., Xu, B., 2009: A real-time 3D scanning system for pavement distortion inspection. Measurement Science and Technology 21(1): 015702. http://dx.doi.org/10.1088/0957-0233/21/1/015702

Lee, J., Nam, B., Abdel-Aty, M., 2015: Effects of pavement surface conditions on traffic crash severity. Journal of Transportation Engineering 141(10): 04015020. https://doi.org/10.1061/(ASCE)TE.1943-5436.0000785

Morgado, J., Neves, J., 2014: Work zone planning in pavement rehabilitation: Integrating cost, duration, and user effects. Journal of Construction Engineering and Management 140(11): 04014050. https://doi.org/10.1061/(ASCE)CO.1943-7862.0000888

Paterson, W.D., 1987: Road deterioration and maintenance effects: Models for planning and management.

Săceanu, C., 2013: Forest roads degradation in correlation with traffic characteristics. Proceedings of the Biennial International Symposium, Forest and Sustainable Development, Brașov, Romania, 19–20th October 2012. Transilvania University of Brasov.

Talbot, B., Rahlf, J., Astrup, R., 2018: An operational UAV-based approach for stand-level assessment of soil disturbance after forest harvesting. Scandinavian Journal of Forest Research 33(4): 387–396. https://doi.org/10.1080/02827581.2017.1418421

Tighe, S., Haas, R., Ponniah, J., 2003: Life-cycle cost analysis of mitigating reflective cracking. Transportation Research Record 1823(1): 73–79. https://doi.org/10.3141/1823-09

Tsai, Y.J., Li, F., Wu, Y., 2013: A new rutting measurement method using emerging 3D line-laser-imaging system. International Journal of Pavement Research and Technology 6(5): 667. https://doi.org/10.6135/ijprt.org.tw/2013.6(5).667

Türk, Y., Aydın, A., Eker, R., Bodur, M., 2018: Evaluation of UAV Usage Possibility in Determining the Environmental Impacts of Construction Activities of Forest Roads: Preliminary Results. In Proceedings of International Ecology 2018 Symposium, 469 p.

Türk, Y., Boz, F., Aydın, A., Eker, R., 2019a:. Evaluation of UAV usage possibility in determining the forest road pavement degradation: preliminary results. In Proceedings of 3rd International Engineering Research Symposium, 630–633 p.

Türk, Y., Aydın, A., Eker, R., 2019b: Effectiveness of open top culverts in forest road deformations: preliminary results from a forest road section, Düzce-Turkey. In Proceedings of 2nd International Symposium of Forest Engineering and Technologies, 147–152 p.

Türk, Y., Canyurt, H., Eker, R., Aydın, A., 2022a: Determination of forest road cut and fill volumes by using un-manned aerial vehicle: A case study in the Bolu-Taşlıyayla. Turkish Journal of Forestry Research (special issue): 97–104. https://doi.org/10.17568/ogmoad.1093695

Türk, Y., Aydın, A., Eker, R., 2022b: Comparison of Autonomous and Manual UAV Flights in Determining Forest Road Surface Deformations. European Journal of Forest Engineering 8(2): 77–84. https://doi.org/10.33904/ejfe.1206846

Türk, Y., Özçelik, V., Akduman, E., 2024: Capabilities of using UAVs and close range photogrammetry to determine short-term soil losses in forest road cut slopes in semi-arid mountainous areas. Environ Monit Assess 196(2): 149. https://doi.org/10.1007/s10661-024-12339-1

Ulvi, A., 2018: Analysis of the utility of the unmanned aerial vehicle (UAV) in volume calculation by using photogrammetric techniques. International Journal of Engineering and Geosciences 3(2): 43–49. https://doi.org/10.26833/ijeg.377080

Wang, H., 2005: Development of laser system to measure pavement rutting.

Wang, K.C., Gong, W., Tracy, T., Nguyen, V., 2011: Automated survey of pavement distress based on 2D and 3D laser images. No. MBTC DOT 3023. Mack-Blackwell National Rural Transportation Study Center (US).

Wee, S.Y., Teo, H.W., 2009: Potential modeling of pavement deterioration rate due to cracking. Journal of Civil Engineering, Science and Technology 1(1): 1–6. https://doi.org/10.33736/jcest.62.2009

Yilmaz, H.M., Yakar, M., Mutluoglu, O., Kavurmaci, M.M., Yurt, K., 2012: Monitoring of soil erosion in Cappadocia Region (Selime-Aksaray-Turkey). Environmental Earth Sciences 66: 75–81.

Yakar, M., Ulvi, A., Yiğit, A.Y., Alptekin, A., 2023: Discontinuity set extraction from 3D point clouds obtained by UAV Photogrammetry in a rockfall site. Survey Review 55(392): 416–428. https://doi.org/10.1080/00396265.2022.2119747

Yurtseven, H., Akgul, M., Akay, A.O., Akburak, S., Cigizoglu, H.K., Demir, M., Ozturk, T., Eksi, M., 2019: High accuracy monitoring system to estimate forest road surface degradation on horizontal curves Environ. Monit. Assess. 191: 1–17. https://doi.org/10.1007/s10661-018-7155-8

Zhang, C., 2008: Development of a UAV-based remote sensing system for unpaved road condition assessment. Proceedings of American Society for Photogrammetry and Remote Sensing Annual Conference. Portland.

Authors' addresses:

Assoc. prof. Yılmaz Türk, PhD *
e-mail: yilmazturk@duzce.edu.tr
Prof. Abdurrahim Aydın, PhD
e-mail: aaydin@duzce.edu.tr
Düzce University
Faculty of Forestry
Department of Forest Engineering
81620 Düzce
TÜRKİYE

Assis. prof. Remzi Eker, PhD
e-mail: remzi.eker@ikc.edu.tr
İzmir Katip Çelebi University
Faculty of Forestry
Department of Forest Engineering
35620 İzmir
TÜRKİYE

* Corresponding author